

42. G. H. Denton *et al.*, *Geogr. Ann. Ser. A Phys. Geogr.* **81A**, 107 (1999).
43. A 35-cm interval in RC11-83, which has an average sedimentation rate through this section of 24 cm/1000 years [a 29-cm interval in RC11-83 (19, 20)], would correspond to a time period of 1450 years.
44. W. F. Ruddiman, *Quat. Sci. Rev.* **22**, 1597 (2003).
45. Most Nd and carbon isotope measurements in the deglacial and Bølling warming portion of the record were not made on the same sample depths or splits. We therefore conservatively confine our interpretations to lead-lag relationships >150 years or >3 cm of core length.
46. S. B. Jacobsen, G. J. Wasserburg, *Earth Planet. Sci. Lett.* **50**, 139 (1980).
47. J. Jouzel *et al.*, *Nature* **329**, 403 (1987).
48. D. J. Piepgras, S. B. Jacobsen, *Geochim. Cosmochim. Acta* **52**, 1373 (1988).
49. D. J. Piepgras, G. J. Wasserburg, *Geochim. Cosmochim. Acta* **51**, 1257 (1987).
50. C. Jeandel, *Earth Planet. Sci. Lett.* **117**, 581 (1993).
51. D. Hodell, K. A. Venz, C. D. Charles, U. S. Ninnemann, *Geochim. Geophys. Geosyst.* **4**, 1 (2003).
52. D. G. Martinson *et al.*, *Quat. Res.* **27**, 1 (1987).
53. This manuscript benefited from discussions with R. Anderson, S. Barker, W. Broecker, H. Elderfield, E. Martin, J. McManus, U. Ninnemann, H. Scher, and A. Tripati; laboratory assistance from D. Zylberberg; and comments by anonymous reviewers. This study was supported by NSF grants OCE 98-09253 and OCE

00-96427 to S.L.G. and S.R.H. and ATM03-27722 and OCE99-11637 to R.G.F. Samples used in this project were provided by the Lamont-Doherty Earth Observatory Deep-Sea Sample Repository, supported by the NSF (grant OCE 00-02380) and the Office of Naval Research (grant N00014-02-1-0073). This is LDEO Contribution #6702.

## Supporting Online Material

www.sciencemag.org/cgi/content/full/307/5717/1933/DC1  
Tables S1 and S2

7 September 2004; accepted 31 January 2005  
10.1126/science.1104883

# REPORTS

## A New Population of Very High Energy Gamma-Ray Sources in the Milky Way

F. Aharonian,<sup>1</sup> A. G. Akhperjanian,<sup>2</sup> K.-M. Aye,<sup>3</sup> A. R. Bazer-Bachi,<sup>4</sup> M. Beilicke,<sup>5</sup> W. Benbow,<sup>1</sup> D. Berge,<sup>1</sup> P. Berghaus,<sup>6\*</sup> K. Bernlöhr,<sup>1,7</sup> C. Boisson,<sup>8</sup> O. Bolz,<sup>1</sup> C. Borgmeier,<sup>7</sup> I. Braun,<sup>1</sup> F. Breitling,<sup>7</sup> A. M. Brown,<sup>3</sup> J. Bussons Gordo,<sup>9</sup> P. M. Chadwick,<sup>3</sup> L.-M. Chouet,<sup>10</sup> R. Cornils,<sup>5</sup> L. Costamante,<sup>1</sup> B. Degrange,<sup>10</sup> A. Djannati-Atai,<sup>6</sup> L. O'C. Drury,<sup>11</sup> G. Dubus,<sup>10</sup> T. Ergin,<sup>7</sup> P. Espigat,<sup>6</sup> F. Feinstein,<sup>9</sup> P. Fleury,<sup>10</sup> G. Fontaine,<sup>10</sup> S. Funk,<sup>1†</sup> Y. A. Gallant,<sup>9</sup> B. Giebels,<sup>10</sup> S. Gillessen,<sup>1</sup> P. Goret,<sup>12</sup> C. Hadjichristidis,<sup>3</sup> M. Hauser,<sup>13</sup> G. Heinzelmann,<sup>5</sup> G. Henri,<sup>14</sup> G. Hermann,<sup>1</sup> J. A. Hinton,<sup>1</sup> W. Hofmann,<sup>1</sup> M. Holleran,<sup>15</sup> D. Horns,<sup>1</sup> O. C. de Jager,<sup>15</sup> I. Jung,<sup>1,13‡</sup> B. Khélifi,<sup>1</sup> Nu. Komin,<sup>7</sup> A. Konopelko,<sup>1,7</sup> I. J. Latham,<sup>3</sup> R. Le Gallou,<sup>4</sup> A. Lemièrre,<sup>6</sup> M. Lemoine,<sup>10</sup> N. Leroy,<sup>10</sup> T. Lohse,<sup>7</sup> A. Marcowith,<sup>4</sup> C. Masterson,<sup>1</sup> T. J. L. McComb,<sup>3</sup> M. de Naurois,<sup>16</sup> S. J. Nolan,<sup>3</sup> A. Noutsos,<sup>3</sup> K. J. Orford,<sup>3</sup> J. L. Osborne,<sup>3</sup> M. Ouchrif,<sup>16</sup> M. Panter,<sup>1</sup> G. Pelletier,<sup>14</sup> S. Pita,<sup>6</sup> G. Pühlhofer,<sup>1,13</sup> M. Punch,<sup>6</sup> B. C. Raubenheimer,<sup>15</sup> M. Raue,<sup>5</sup> J. Raux,<sup>16</sup> S. M. Rayner,<sup>3</sup> I. Redondo,<sup>10§</sup> A. Reimer,<sup>17</sup> O. Reimer,<sup>17</sup> J. Ripken,<sup>5</sup> L. Rob,<sup>18</sup> L. Rolland,<sup>16</sup> G. Rowell,<sup>1</sup> V. Sahakian,<sup>2</sup> L. Sauge,<sup>14</sup> S. Schlenker,<sup>7</sup> R. Schlickeiser,<sup>17</sup> C. Schuster,<sup>17</sup> U. Schwanke,<sup>7</sup> M. Siewert,<sup>17</sup> H. Sol,<sup>8</sup> R. Steenkamp,<sup>19</sup> C. Stegmann,<sup>7</sup> J.-P. Tavernet,<sup>16</sup> R. Terrier,<sup>6</sup> C. G. Théoret,<sup>6</sup> M. Tluczykont,<sup>10</sup> D. J. van der Walt,<sup>15</sup> G. Vasileiadis,<sup>9</sup> C. Venter,<sup>15</sup> P. Vincent,<sup>16</sup> B. Visser,<sup>15</sup> H. J. Völk,<sup>1</sup> S. J. Wagner<sup>13</sup>

Very high energy  $\gamma$ -rays probe the long-standing mystery of the origin of cosmic rays. Produced in the interactions of accelerated particles in astrophysical objects, they can be used to image cosmic particle accelerators. A first sensitive survey of the inner part of the Milky Way with the High Energy Stereoscopic System (HESS) reveals a population of eight previously unknown firmly detected sources of very high energy  $\gamma$ -rays. At least two have no known radio or x-ray counterpart and may be representative of a new class of "dark" nucleonic cosmic ray sources.

Very high energy (VHE)  $\gamma$ -rays with energies  $E > 10^{11}$  eV are probes of the nonthermal universe, providing access to energies far greater than those that can be produced in

accelerators on Earth. The acceleration of electrons or nuclei in astrophysical sources leads inevitably to the production of  $\gamma$ -rays by the decay of  $\pi^0$ s produced in hadronic inter-

actions, inverse Compton scattering of high-energy electrons on background radiation fields, or the nonthermal bremsstrahlung of energetic electrons. Several classes of objects in the Galaxy are suspected or known particle accelerators: pulsars and their pulsar wind

<sup>1</sup>Max-Planck-Institut für Kernphysik, Post Office Box 103980, D-69029 Heidelberg, Germany. <sup>2</sup>Yerevan Physics Institute, 2 Alikhanian Brothers Street, 375036 Yerevan, Armenia. <sup>3</sup>Department of Physics, University of Durham, South Road, Durham DH1 3LE, UK. <sup>4</sup>Centre d'Etude Spatiale des Rayonnements, CNRS/UPS, 9 av. du Colonel Roche, BP 4346, F-31029 Toulouse Cedex 4, France. <sup>5</sup>Institut für Experimentalphysik, Universität Hamburg, Luruper Chaussee 149, D-22761 Hamburg, Germany. <sup>6</sup>Physique Corpusculaire et Cosmologie, IN2P3/CNRS, Collège de France, 11 Place Marcelin Berthelot, F-75231 Paris Cedex 05, France. <sup>7</sup>Institut für Physik, Humboldt-Universität zu Berlin, Newtonstr. 15, D-12489 Berlin, Germany. <sup>8</sup>Laboratoire Univers et Théories (LUTH), UMR 8102 du CNRS, Observatoire de Paris, Section de Meudon, F-92195 Meudon Cedex, France. <sup>9</sup>Groupe d'Astroparticules de Montpellier, IN2P3/CNRS, Université Montpellier II, CC85, Place Eugène Bataillon, F-34095 Montpellier Cedex 5, France. <sup>10</sup>Laboratoire Leprince-Ringuet, IN2P3/CNRS, Ecole Polytechnique, F-91128 Palaiseau, France. <sup>11</sup>Dublin Institute for Advanced Studies, 5 Merrion Square, Dublin 2, Ireland. <sup>12</sup>Service d'Astrophysique, DAPNIA/DSM/CEA, CE Saclay, F-91191 Gif-sur-Yvette, France. <sup>13</sup>Landessternwarte, Königstuhl, D-69117 Heidelberg, Germany. <sup>14</sup>Laboratoire d'Astrophysique de Grenoble, INSU/CNRS, Université Joseph Fourier, BP 53, F-38041 Grenoble Cedex 9, France. <sup>15</sup>Unit for Space Physics, North-West University, Potchefstroom 2520, South Africa. <sup>16</sup>Laboratoire de Physique Nucléaire et de Hautes Energies, IN2P3/CNRS, Universités Paris VI and VII, 4 Place Jussieu, F-75231 Paris Cedex 05, France. <sup>17</sup>Institut für Theoretische Physik, Lehrstuhl IV: Weltraum und Astrophysik, Ruhr-Universität Bochum, D-44780 Bochum, Germany. <sup>18</sup>Institute of Particle and Nuclear Physics, Charles University, V Holesovickach 2, 180 00 Prague 8, Czech Republic. <sup>19</sup>University of Namibia, Private Bag 13301, Windhoek, Namibia.

\*Present address: Université Libre de Bruxelles, Faculté des Sciences, Campus de la Plaine, CP230, Boulevard du Triomphe, 1050 Bruxelles, Belgium.

†To whom correspondence should be addressed. E-mail: stefan.funk@mpi-hd.mpg.de

‡Present address: Department of Physics, Washington University, 1 Brookings Drive, CB 1105, St. Louis, MO 63130, USA.

§Present address: Department of Physics and Astronomy, University of Sheffield, Hicks Building, Hounsfield Road, Sheffield S3 7RH, UK.

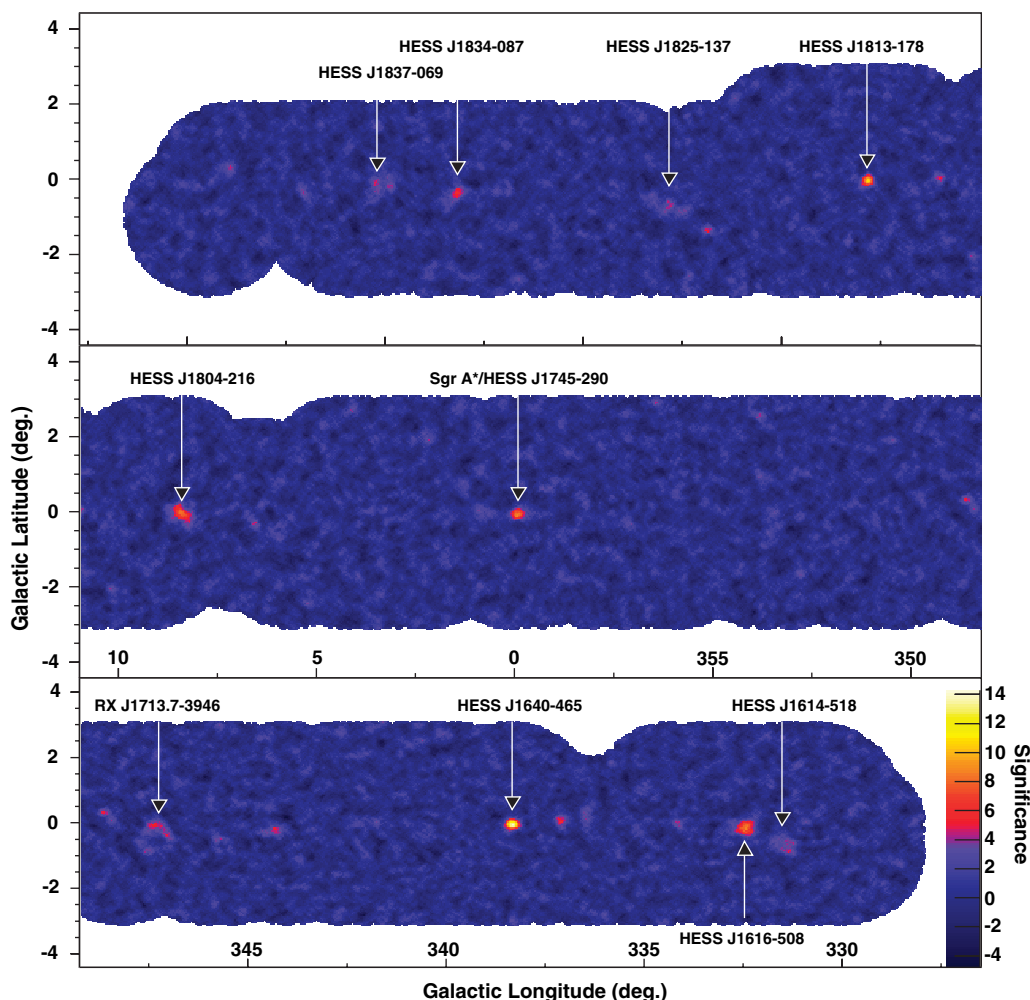


**Fig. 1.** Significance map of the HESS 2004 galactic plane scan. Reobservations of candidates from the initial scan are included here. The background level was estimated using a ring around the test source position (12). On-source counts are summed over a circle of radius  $\theta$ , where  $\theta = 0.14^\circ$ , a cut appropriate for point-like sources. To calculate the significance, it is necessary to correct for the relative acceptance and area of the on and off regions. The correction is given by a runwise radially symmetric acceptance function, which describes the background at the 1% level. Events falling up to  $2^\circ$  from the pointing direction of the system are used. At this angle, the  $\gamma$ -ray acceptance efficiency has decreased to 20% of its peak value. After acceptance correction, the approach of Li and Ma (30) is used to calculate the significance at every point on the map. We note that consistent results are obtained for these eight sources with the use of a completely independent calibration and analysis chain (31).

nebulae (PWNs), supernova remnants (SNRs), microquasars, and massive star-forming regions. VHE  $\gamma$ -ray sources that have been detected in the Galaxy include PWNs, SNRs, and objects with no identified counterpart at other energies. Such sources without counterpart are particularly interesting, because a lack of x-ray emission could indicate that the primary accelerated particles are nucleons rather than high-energy electrons. Essentially all potential galactic sources cluster along the galactic plane. Thus, a systematic survey of the galactic plane is the best means to investigate the properties of these source classes and to search for currently unknown types of galactic VHE  $\gamma$ -ray emitters.

Large-scale  $\gamma$ -ray surveys in the TeV energy regime ( $1 \text{ TeV} = 10^{12} \text{ eV}$ ) have been performed using the Milagro water-Cherenkov detector (1) and the Tibet air-shower array (2). These all-sky instruments have only modest sensitivity, reaching a flux limit comparable to the flux level of the Crab Nebula,  $\sim 2 \times 10^{-11} \text{ cm}^{-2} \text{ s}^{-1}$  (for  $E > 1 \text{ TeV}$ ), in 1 year of observations. Both surveys covered  $\sim 2\pi$  steradians of the northern sky and resulted only in flux upper limits. A survey of

the part of the galactic plane accessible from the Northern Hemisphere ( $-2^\circ < l < 85^\circ$ , where  $l$  denotes galactic longitude) was performed by the stereoscopic High Energy Gamma Ray Astronomy (HEGRA) array of imaging Cherenkov telescopes (3). No sources of VHE  $\gamma$ -rays were found in this survey, but upper limits between 15% of the Crab flux for galactic longitudes  $l > 30^\circ$  and more than 30% of the Crab flux in the inner part of the Milky Way were derived (4). Until the completion of the High Energy Stereoscopic System (HESS) (5) in early 2004, no VHE  $\gamma$ -ray survey of the southern sky or of the central region of the Galaxy had been performed. The central part of the Galaxy contains the highest density of potential  $\gamma$ -ray sources. We conducted a survey of this region with HESS in 2004, at a flux sensitivity of 3% of the Crab flux.

HESS is an array of telescopes exploiting the imaging Cherenkov technique. The telescopes image the Cherenkov light emitted by atmospheric particle cascades initiated by  $\gamma$ -rays or cosmic rays in the upper atmosphere. Measurements of the same cascade by multiple telescopes allow improved rejection of the cosmic-ray background and better angular

and energy resolution relative to single-dish telescopes. HESS consists of four atmospheric Cherenkov telescopes, each with  $107 \text{ m}^2$  of mirror area (6) and equipped with a 960-pixel photomultiplier tube camera (7). The four telescopes are operated in a stereoscopic mode with a system trigger (8), requiring at least two telescopes to provide images of each cascade. HESS has the largest field of view (diameter  $5^\circ$ ) of all imaging Cherenkov telescopes now in operation, which yields a considerable advantage for surveys (9).

HESS provides unprecedented sensitivity to  $\gamma$ -rays above 100 GeV, below 1% of the flux from the Crab Nebula, for long exposures. This sensitivity has already been demonstrated by high-significance detections of the galactic center (HESS J1745-290) (10) and the SNR RX J1713.7-3946 (11). The angular resolution for individual  $\gamma$ -rays is better than  $0.1^\circ$ , allowing a source position error of 30 arc sec to be achieved even for relatively faint sources.

We scanned the inner part of the galactic plane (galactic longitude  $-30^\circ < l < 30^\circ$  and latitude  $-3^\circ < b < 3^\circ$ ) with HESS from May to July 2004. Observations 28 min in duration

were made in steps of 0.7° in longitude and steps of 1° in latitude for a total observation time of 112 hours. An average 5-standard-deviation detection sensitivity of  $3 \times 10^{-11}$  photons  $\text{cm}^{-2} \text{s}^{-1}$  above 100 GeV (~3% of the Crab Flux) was reached for points on the galactic plane. Seven promising candidate sources from the survey were reobserved from July to September for typically 3.5 hours per source.

Eight unknown VHE sources were detected at the level of >6 standard deviations after accounting for all trial factors (Fig. 1 and Table 1). The known VHE sources HESS J1745-290 (at the galactic center) and RX J1713.7-3946 were also detected in the scan data. The analysis used the standard HESS analysis procedure, optimized for point-like sources (12).

The significance values shown in Fig. 1 (and  $S^3$  in Table 1) do not directly reflect the probability that a given signal represents a  $\gamma$ -ray source, because the large number of search points in the sky map (250,000) enhances the chance for statistical fluctuations to mimic a signal. Probabilities must be scaled by a trial factor accounting for the number of attempts to find a source, here conservatively assumed to be equal to the number of points in the sky map. Simulations of randomly generated sky maps without  $\gamma$ -ray sources show that the effective number of trials is smaller than the number of points because of correlations between adjacent search points, which are more closely spaced than the instrumental width of the point spread function. Trial factors apply only for the initial search, where source candidates were identified ( $S^1$ , before trials), but not for follow-up observations, where the significance ( $S^2$ ) of a signal was evaluated assuming the position derived from the initial search. The scaled-down significance from the initial search and the result of the follow-up observations were combined by summation in quadrature to give a final detection significance ( $S^4$ ).

Because most sources appear moderately extended,  $S^5$  in Table 1 lists the significance similar to  $S^4$  but assuming extended sources. For each of these candidates, a spectral analysis was performed, and Table 1 also gives the best fit flux above 200 GeV.

For the purpose of source size and position fitting, an additional cut requiring an image size exceeding 200 photoelectrons in each camera was applied. This cut further suppresses the cosmic-ray background (by a factor of ~7) at the expense of reduced statistical significance and increased energy threshold (250 GeV). It also improves the angular resolution by 30%. After applying this cut, the spatial distribution of excess events for each candidate was fit to a model of a two-dimensional Gaussian  $\gamma$ -ray emission region (Table 1) convolved with the point spread function of the instrument (derived from Monte Carlo simulations and verified by observations of the Crab Nebula).

The new galactic VHE  $\gamma$ -ray emitters cluster close to the galactic plane, with a mean  $b$  of  $-0.25^\circ$  and a root mean square (rms) of  $0.25^\circ$  (Fig. 2). This is a clear indication that we see a population of galactic (rather than extragalactic) sources. Furthermore, the observed distribution resembles that of galactic SNRs (13) and of energetic pulsars ( $\dot{E} > 10^{34}$  erg/s) (14). However, because of the nonuniform exposure of the scan and the unknown luminosity distribution of the parent population, we cannot make a quantitative statement about the compatibility of these distributions.

All of the sources are significantly extended beyond the size of the HESS point spread function. Given that the search described here

was optimized for point-like sources, it is likely that several more significant sources with an extended nature exist in this data set. We note that the new sources mostly have spectra with rather hard photon indices in the range between that expected for SNRs and that of the Crab Nebula.

We have searched for counterparts for the new  $\gamma$ -ray sources in other wavelength bands. Fig. 3 shows the  $\gamma$ -ray emission from the region around each source together with potential counterparts. Although the chance probability for spatial coincidences with SNRs in the region of the scan is not negligible (6%), plausible associations exist for three of the new sources—HESS J1640-465, HESS J1834-087, and HESS J1804-216—with an SNR.

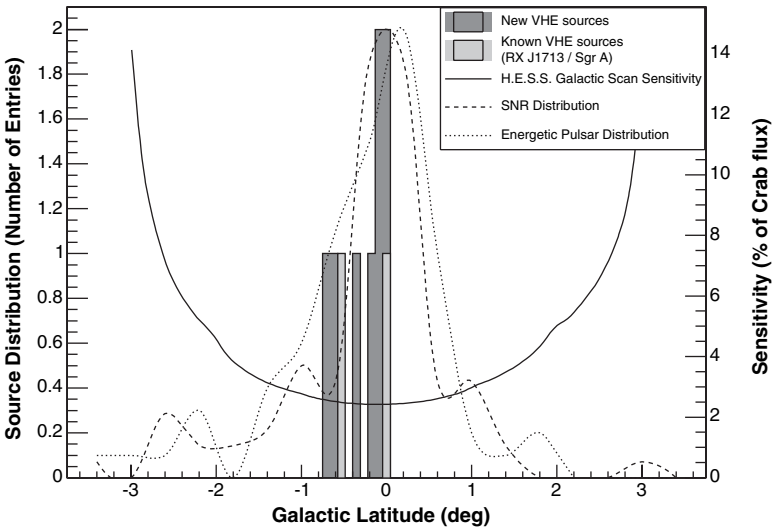


**Fig. 2.** Latitude distribution of the eight new VHE  $\gamma$ -ray sources (and two known sources in the scan region), along with the average sensitivity of the HESS galactic plane scan (for a  $5\sigma$  detection, expressed as a percentage of the flux from the Crab Nebula). The distributions of galactic SNRs and of energetic pulsars (including only pulsars with spin-down luminosity  $\dot{E}$  more than  $10^{34}$  erg/s) are shown for comparison; for both distributions, only objects within the longitude range of the HESS survey ( $-30^\circ < l < 30^\circ$ ) were selected.

**Table 1.** Characteristics of the new  $\gamma$ -ray sources. Position: galactic longitude ( $l$ ) and latitude ( $b$ ) with a statistical error in the range of 1 to 2 arc min. Size: estimated source extension  $\sigma$  for a brightness distribution of the form  $\rho \propto \exp(-r^2/2\sigma^2)$  with a statistical error in the range of 10 to 30%.  $S_1$ : Significance for a point source cut of  $\theta^2 = (0.14^\circ)^2$ , using scan data only, without correction for the number of trials.  $S_2$ : As for  $S_1$  but only including follow-up observations of this source (no correction needed).  $S_3$ : Significance of combined scan and follow-up observations (as shown in Fig. 1).  $S_4$ : As for  $S_3$  but including a correction for the number of trials ( $n = 250,000$ ).  $S_5$ : As for  $S_4$  but with an extended cut of  $\theta^2 = (0.22^\circ)^2$ . Flux: Estimated flux above 200 GeV ( $\times 10^{-12} \text{ cm}^{-2} \text{s}^{-1}$ ) with a statistical error of 10 to 35%.

Name	Position		Size $\sigma$ (arc min)	Significance					Flux
	$l$	$b$		$S_1$	$S_2$	$S_3$	$S_4$	$S_5$	
HESS J1614-518*	331.54°	-0.59°	12	5.2	4.3	6.7	4.7	6.8	9
HESS J1616-508	332.40°	-0.15°	11	7.4	8.9	11.6	10.5	12.8	17
HESS J1640-465	338.32°	-0.02°	2	11.7	8.3	14.3	13.4	11.5	19
HESS J1804-216	8.44°	-0.05°	13	8.2	5.9	10.1	8.8	9.6	16
HESS J1813-178	12.81°	-0.03°	3	10.2	8.3	13.2	12.2	8.9	12
HESS J1825-137*	17.78°	-0.72°	10	4.4	3.7	5.8	3.7	6.5	9
HESS J1834-087	23.28°	-0.34°	12	6.7	5.6	8.7	7.2	7.8	13
HESS J1837-069	25.21°	-0.12°	4	6.0	6.0	8.4	6.9	6.4	9

\*These sources were reobserved within the field of view of dedicated observations of another target.

HESS J1640-465 is spatially coincident with the SNR G338.3-0.0, which is a broken-shell SNR lying on the edge of a bright ultracompact H II region (13). This H II region could conceivably provide target material for nuclear particles accelerated in the SNR, generating VHE  $\gamma$ -rays by  $\pi^0$  decay. The unidentified Energetic Gamma Ray Experiment Telescope (EGRET) source 3EG J1639-4702 (15) lies 35 arc min away and could also be connected to HESS J1640-465, given the position uncertainty of 34 arc min of the EGRET source. HESS J1834-087 is spatially coincident with the SNR G23.3-0.3 (W41), a shell-type SNR of diameter 27 arc min (16). HESS J1804-216 coincides with the southwestern rim of the shell-type SNR G8.7-0.1 (W30) of radius 26 arc min. From CO observations (17), the surrounding region is known to be associated with molecular gas where massive star formation is taking place. This SNR could be associated with the nearby (25 arc min) young pulsar PSR J1803-2137 (18).

HESS J1804-216 is one of three plausible associations with nebulae powered by sufficiently energetic young pulsars. The others are HESS J1825-137 and HESS J1616-508. HESS J1825-137 lies 13 arc min from the pulsar PSR J1826-1334, which has been associated with the nearby unidentified EGRET source 3EG J1826-1302 (19). A diffuse emission region, 5 arc min in diameter and extending asymmetrically to the south of the pulsar, was detected using the XMM (X-ray Multi-Mirror Mission) x-ray telescope (20). This diffuse emission is interpreted as synchrotron emission produced by a PWN. The VHE emission is similarly located south of PSR J1826-1334 and could be coincident with the PWN. The conversion efficiency implied from spin-down power to VHE  $\gamma$ -rays is less than 1%. HESS J1616-508 is located in the middle of a complicated region 9 arc min from the young hard x-ray pulsar PSR J1617-5055 (21). The VHE  $\gamma$ -ray flux is again less than 1% of the spin-down luminosity of the

pulsar. The SNR G332.4-0.4 (RCW 103) (13), which harbors a compact x-ray source (1E 161348-5055) (22), lies 13 arc min away, as does the SNR G332.4+0.1 (Kes 32) (23), but neither of these SNRs is spatially coincident with the VHE emission. (Note that none of the discussed SNR or PWN associations currently meet the criteria necessary for promotion to counterparts. Counterpart identification requires positional agreement with an identified source, a plausible  $\gamma$ -ray emission mechanism, and consistent multi-frequency behavior.)

For HESS J1837-069 a potential counterpart is the diffuse hard x-ray source G25.5+0.0, which is 12 arc min across and was detected in the Advanced Satellite for Cosmology and Astrophysics (ASCA) galactic plane survey (24). The nature of this bright x-ray source is unclear, but it may be an x-ray synchrotron emission-dominated SNR such as SN 1006 or a PWN. The brightest feature in the ASCA map (AX J1838.0-0655), located

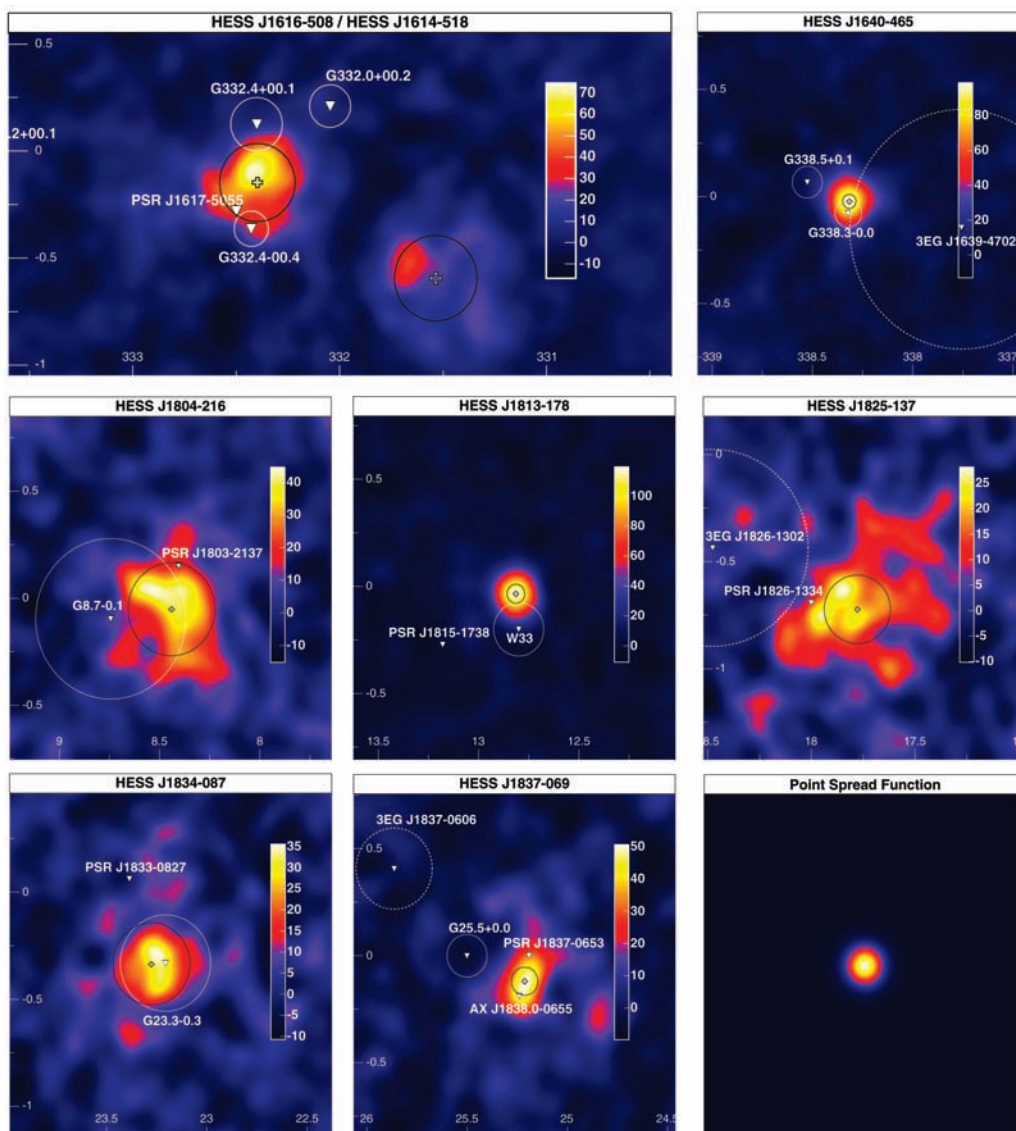


**Fig. 3.** Smoothed excess maps in units of counts of the regions around each of the eight new sources in galactic coordinates (in degrees). An image size cut ( $>200$  photoelectrons) has been applied to reduce the background level and improve the angular resolution. A Gaussian of rms  $0.05^\circ$  is used for smoothing to reduce the impact of statistical fluctuations. The best fit centroids for the  $\gamma$ -ray emission are shown as crosses, and the best fit rms size as a black circle. Possible counterparts are marked by white triangles, with circles indicating the nominal source radius (or the position error in the case of EGRET sources). The lower right panel indicates the simulated point spread function of the instrument for these data, smoothed in the same way as the other panels.

south of G25.5+0.0, coincides with the center of gravity of the VHE emission and is therefore the most promising counterpart candidate. This still unidentified source was also serendipitously detected by the BeppoSAX x-ray satellite instrument and also in the hard x-ray (20 to 100 keV) band in the galactic plane survey performed with the Integral (International Gamma-Ray Astrophysics Laboratory) satellite (25).

For the two remaining sources, HESS J1813-178 and HESS J1614-518, no plausible counterparts have been found at other wavelengths. HESS J1813-178 is not spatially coincident with any counterparts in the region but lies 10 arc min from the center of the radio source W 33. W 33 extends over 15 arc min, with a compact radio core (G12.8-0.2) that is 1 arc min across (26). The region is highly obscured and has indications of recent star formation (27). In its extended emission and location close to an association of hot O and B stars, HESS J1813-178 resembles the unidentified TeV source discovered by HEGRA, TeV J2032+4130 (28), and the first HESS unidentified  $\gamma$ -ray source, HESS J1303-63 (29). HESS J1614-518 has no plausible SNR or pulsar counterpart. This source is in the field of view of HESS J1616-508, which is located nearby ( $\sim 1^\circ$  away). The lack of any counterparts for these two sources suggests the exciting possibility of a new class of "dark" particle accelerators in the Galaxy.

In conclusion, we have on the basis of the survey generated an unbiased catalog of VHE  $\gamma$ -ray sources in the central region of our Galaxy, extending our multiwavelength knowledge of the Milky Way into the VHE domain. Three of the eight newly discovered sources are potentially associated with SNRs, two with EGRET sources. In three cases an association with pulsar-powered nebulae is not excluded. At least two sources have no identified counterpart in radio or x-rays, which suggests the exciting possibility of a new class of "dark" nucleonic particle accelerators. This catalog provides insights into particle acceleration in our Galaxy and adds a piece to the long-standing puzzle of cosmic-ray origin.

#### References and Notes

1. R. Atkins *et al.*, *Astrophys. J.* **608**, 680 (2004).
2. M. Amenomori *et al.*, *Astrophys. J.* **580**, 887 (2002).
3. A. Daum *et al.*, *Astropart. Phys.* **8**, 1 (1997).
4. F. Aharonian *et al.*, *Astron. Astrophys.* **395**, 803 (2002).
5. W. Benbow *et al.*, in *International Symposium on High-Energy Gamma-Ray Astronomy*, F. A. Aharonian, H. J. Völk, D. Horns, Eds. (AIP Conference Proceedings 745, 2005), pp. 611–616.
6. K. Bernlöhr *et al.*, *Astropart. Phys.* **20**, 111 (2003).
7. P. Vincent *et al.*, in *Proceedings of the 28th International Cosmic Ray Conference*, T. Kajita *et al.*, Eds. (Universal Academy Press, Tokyo, 2003), pp. 2887–2890.
8. S. Funk *et al.*, *Astropart. Phys.* **22**, 285 (2004).
9. F. Aharonian *et al.*, *Astropart. Phys.* **6**, 369 (1997).
10. F. Aharonian *et al.*, *Astron. Astrophys.* **425**, L13 (2004).
11. F. Aharonian *et al.*, *Nature* **432**, 75 (2004).
12. F. Aharonian *et al.*, *Astron. Astrophys.* **430**, 865 (2005).
13. D. A. Green, *Bull. Astron. Soc. India* **32**, 335 (2004).
14. R. N. Manchester, G. B. Hobbs, A. Teoh, M. Hobbs, *Astron. J.*, in press (available at <http://xxx.lanl.gov/abs/astro-ph/0412641>).
15. R. C. Hartman *et al.*, *Astrophys. J. Suppl. Ser.* **123**, 79 (1999).
16. N. E. Kassim, *Astron. J.* **103**, 943 (1992).
17. L. Blitz, M. Fich, A. A. Stark, *Astrophys. J. Suppl. Ser.* **49**, 183 (1982).
18. N. E. Kassim, *Nature* **343**, 146 (1990).
19. P. L. Nolan, W. F. Tompkins, I. A. Grenier, P. F. Michelson, *Astrophys. J.* **597**, 615 (2003).
20. B. M. Gaensler, N. S. Schulz, V. M. Kaspi, M. J. Pivovarov, W. E. Becker, *Astrophys. J.* **588**, 441 (2003).
21. K. Torii *et al.*, *Astrophys. J.* **494**, L207 (1998).
22. E. V. Gotthelf, R. Petre, U. Hwang, *Astrophys. J.* **487**, L175 (1997).
23. J. Vink, *Astrophys. J.* **604**, 693 (2004).
24. A. Bamba, M. Ueno, K. Koyama, S. Yamauchi, *Astrophys. J.* **589**, 253 (2003).
25. A. Malizia *et al.*, in *Proceedings of the V INTEGRAL Workshop*, Munich, 16 to 20 February 2004 (available at <http://xxx.lanl.gov/abs/astro-ph/0404596>).
26. A. Haschick, P. T. P. Ho, *Astrophys. J.* **267**, 638 (1983).
27. E. Churchwell, *Astron. Astrophys. Rev.* **2**, 79 (1990).
28. F. Aharonian *et al.*, *Astron. Astrophys.* **393**, L37 (2002).
29. M. Beilicke *et al.*, in *International Symposium on High-Energy Gamma-Ray Astronomy*, F. A. Aharonian, H. J. Völk, D. Horns, Eds. (AIP Conference Proceedings 745, 2005), pp. 347–352.
30. T. Li, Y. Ma, *Astrophys. J.* **272**, 317 (1983).
31. M. de Naurois *et al.*, in *Proceedings of the 28th International Cosmic Ray Conference*, T. Kajita *et al.*, Eds. (Universal Academy Press, Tokyo, 2003), pp. 2907–2910.
32. The support of the Namibian authorities and of the University of Namibia in facilitating the construction and operation of HESS is gratefully acknowledged, as is the support of the German Ministry for Education and Research (BMBF), the Max Planck Society, the French Ministry for Research, the CNRS-IN2P3 and the Astroparticle Interdisciplinary Programme of the CNRS, the UK Particle Physics and Astronomy Research Council (PPARC), the Institute of Particle and Nuclear Physics of the Charles University, the South African Department of Science and Technology and National Research Foundation, and the University of Namibia. We appreciate the excellent work of the technical support staff in Berlin, Durham, Hamburg, Heidelberg, Palaiseau, Paris, Saclay, and Namibia in the construction and operation of the equipment. L.C., C.M., M.O., I.R., and M.T. are also affiliated with the European Associated Laboratory for Gamma-Ray Astronomy, jointly supported by CNRS and the Max Planck Society.

13 December 2004; accepted 18 January 2005  
10.1126/science.1108643

## Chemical Detection with a Single-Walled Carbon Nanotube Capacitor

E. S. Snow,\* F. K. Perkins, E. J. Houser, S. C. Badescu, T. L. Reinecke

We show that the capacitance of single-walled carbon nanotubes (SWNTs) is highly sensitive to a broad class of chemical vapors and that this transduction mechanism can form the basis for a fast, low-power sorption-based chemical sensor. In the presence of a dilute chemical vapor, molecular adsorbates are polarized by the fringing electric fields radiating from the surface of a SWNT electrode, which causes an increase in its capacitance. We use this effect to construct a high-performance chemical sensor by thinly coating the SWNTs with chemoselective materials that provide a large, class-specific gain to the capacitance response. Such SWNT chemicapacitors are fast, highly sensitive, and completely reversible.

Sorption-based microsensors are currently a leading candidate for low-power, compact chemical vapor detection for defense, homeland security, and environmental-monitoring applications (1–9). Such sensors combine a nonselective transducer with chemoselective materials that serve as a vapor concentrator, resulting in a highly sensitive detector that responds selectively to a particular class of chemical vapor. An array of such sensors, each coated with a different chemoselective material, produces a response fingerprint that can detect and identify an analyte (1–3). Sorption-based sensors provide sensitive de-

tection for vapors ranging from volatile organic compounds to semivolatile chemical nerve agents, although low-vapor pressure materials such as explosives are challenging because they do not produce a sufficiently high concentration of vapor (4).

The transducer elements for such sensor arrays need to be small, low-power, and compatible with conventional microprocessing technology. Among the choice of transducers are mechanical oscillators that respond to changes in mass (1, 2), chemicapacitors that detect changes in dielectric properties (4–6), and chemiresistors that monitor the resistance of a polymer laced with conductive particles (7–9). Of these transducers, chemicapacitors (4) and chemiresistors (7, 8) are the best suited for low-power sensor arrays. Chemiresistors are simple to implement, but instability of the con-

Naval Research Laboratory, Washington, DC 20375, USA.

\*To whom correspondence should be addressed.  
E-mail: snow@bloch.nrl.navy.mil

---

*This copy is for your personal, non-commercial use only.*

---

**If you wish to distribute this article to others**, you can order high-quality copies for your colleagues, clients, or customers by [clicking here](#).

**Permission to republish or repurpose articles or portions of articles** can be obtained by following the guidelines [here](#).

**The following resources related to this article are available online at [www.sciencemag.org](http://www.sciencemag.org) (this information is current as of May 24, 2015 ):**

**Updated information and services**, including high-resolution figures, can be found in the online version of this article at:

<http://www.sciencemag.org/content/307/5717/1938.full.html>

This article has been **cited by** 121 article(s) on the ISI Web of Science

This article has been **cited by** 28 articles hosted by HighWire Press; see:

<http://www.sciencemag.org/content/307/5717/1938.full.html#related-urls>

This article appears in the following **subject collections**:

Astronomy

<http://www.sciencemag.org/cgi/collection/astronomy>